Original Article

Veterinary Pathology
1-7

DOI: 10.1177/0300985816658100
vet.sagepub.com

Syncytial Hepatitis of Tilapia (*Oreochromis niloticus* L.) is Associated With Orthomyxovirus-Like Virions in Hepatocytes

J. del-Pozo[1], N. Mishra[2], R. Kabuusu[3], S. Cheetham[3], A. Eldar[4], E. Bacharach[5], W. I. Lipkin[2], and H. W. Ferguson[3]

Abstract

Using transmission electron microscopy (TEM), the presented work expands on the ultrastructural findings of an earlier report on "syncytial hepatitis," a novel disease of tilapia (SHT). Briefly, TEM confirmed the presence of an orthomyxovirus-like virus within the diseased hepatocytes but not within the endothelium. This was supported by observing extracellular and intracellular (mostly intraendosomal), 60–100 nm round virions with a trilaminar capsid containing up to 7 electron-dense aggregates. Other patterns noted included enveloped or filamentous virions and virion-containing cytoplasmic membrane folds, suggestive of endocytosis. Patterns atypical for orthymyxovirus included the formation of syncytia and the presence of virions within the perinuclear cisternae (suspected to be the Golgi apparatus). The ultrastructural morphology of SHT-associated virions is similar to that previously reported for tilapia lake virus (TiLV). A genetic homology was investigated using the available reverse transcriptase polymerase chain reaction (RT-PCR) probes for TiLV and comparing clinically sick with clinically normal fish and negative controls. By RT-PCR analysis, viral nucleic acid was detected only in diseased fish. Taken together, these findings strongly suggest that a virus is causally associated with SHT, that this virus shares ultrastructural features with orthomyxoviruses, and it presents with partial genetic homology with TiLV (190 nucleotides).

Keywords

fish, hepatitis, orthomyxovirus, syncytia, tilapia, virus, ultrastructure

Tilapia are considered to be relatively resistant to many of the diseases that beset other farmed fish. Although they are targeted by the usual parasites commonly found in almost any intensively reared fish species and by some bacteria, notably *Streptococcus spp*, viral diseases have not been frequently reported. However, viruses have been recently implicated in several large disease outbreaks with high levels of mortality in both farmed and wild tilapia.[2,8,9,23] These outbreaks featured infection by betanodavirus and herpes-like viruses, causing central nervous system alterations (neuropil vacuolation and meningoencephalitis, respectively), and a novel enveloped RNA-virus causing ocular, cutaneous, and meningeal pathology. A novel cause of tilapia mortality suspected of having a viral etiology is syncytial hepatitis of tilapia (SHT), which has been described in Ecuador.[9] This disease presents grossly with ascites and histologically with hepatocellular lipoprotein accumulation, necrosis, and syncytia formation plus necrosis of gastrointestinal mucosa.[9] Previously described examples of piscine viral diseases that feature hepatic necrosis include infectious salmon anemia (ISA),[24] viral hemorrhagic septicemia in several species,[10,12,19] channel catfish virus,[21] adenovirus-like disease of cultured white sturgeon,[11] and halibut reovirus.[3] Interestingly, the latter also presents with syncytia formation in the liver, which is a feature of SHT.

Our previous report of SHT provided a preliminary description of the clinical presentation, histopathology, and ultrastructural alterations. These included virus-like particles within the cytoplasm of hepatocytes.[9] In this work, we aim to provide additional, detailed information on some of the ultrastructural features of SHT-associated virions using transmission electron microscopy (TEM). Based on ultrastructural similarities, and using reverse transcriptase polymerase chain reaction (RT-PCR), we also set out to test the hypothesis that the virions noted in SHT may have genetic homology with those of tilapia lake virus (TiLV).

[1]Department of Veterinary Pathology, Royal (Dick) School of Veterinary Studies, University of Edinburgh, Edinburgh, UK
[2]Columbia University, New York, NY, USA
[3]St George's University, St Georges, Grenada
[4]The Kimron Veterinary Institute, Bet Dagan, Italy
[5]Tel Aviv University, Tel Aviv, Israel

Corresponding Author:
J. del-Pozo, Department of Veterinary Pathology, Royal (Dick) School of Veterinary Studies, University of Edinburgh, Roslin, EH25 9RG, UK.
Email: jorge.del.pozo@ed.ac.uk

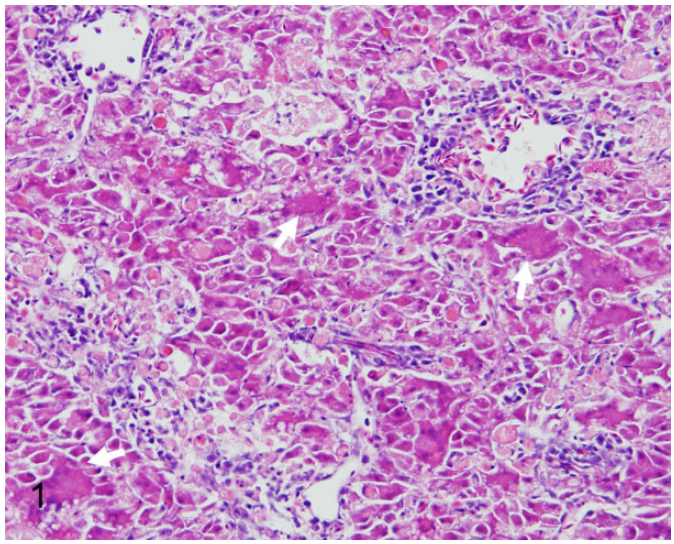

Figure 1. Syncytial hepatitis of tilapia (SHT). There are multifocal to coalescing areas of necrosis, frequent single hepatocellular necrosis with dissociation, syncytial cell formation (white arrows), and perivenular, lymphocytic, inflammatory infiltration. Hematoxylin & eosin (HE).

Materials and Methods

Fish

Details of the clinical presentation of these fish have been previously reported.[9] Briefly, intensively reared tilapia fingerlings (*Oreochromis niloticus* L.) were collected for diagnostic workup following several months of above-normal mortality. In the involved farm, only the own farm-bred tilapia "Chitralada" were affected (with up to 90% mortality), whereas cohabiting tilapia from an outsourced, genetically all-male strain were not affected (basal mortality levels). Typically, clinical disease started shortly after transferring the fish into larger on-growing ponds; at that time, the average fish weight was approximately 3 g.

Case Definition

Grossly, these fish presented with darkening, exophthalmia, and ascites (clear fluid). The livers were grossly unremarkable. Histopathological lesions included necrotizing hepatitis with distinctive hepatocellular syncytial giant cell formation, and necrosis of gastric glandular epithelium and intestinal enterocytes (Fig. 1).

Transmission Electron Microscopy

Ten fish consistent with the gross case definition were anesthetized with clove oil, and the liver was dissected. Half of the liver was fixed in 10% neutral-buffered formalin (NBF) and the other half fixed in 2.5% glutaraldehyde in a 0.1 mol/L sodium cacodylate buffer. The NBF sample was processed for histology to confirm the presence of the histological case definition, which was confirmed in all 10 fish. Samples fulfilling the case definition were selected for subsequent processing for TEM. Specimens destined for TEM were post-fixed in 1% osmium tetroxide in 0.1 mol/L sodium cacodylate for 45 minutes, then washed in three 10-minute changes of 0.1 mol/L sodium cacodylate buffer. These samples were then dehydrated in 50%, 70%, 90%, and 100% normal grade acetones for 10 minutes each, then for a further two 10-minute changes in AnalaR acetone (VWR International, UK). Samples were then embedded in Araldite resin (Electron Microscope Sciences, UK). Sections, 1-µm-thick, were cut on a Reichert OMU4 ultramicrotome (Leica, UK), stained with toluidine blue, and viewed in a light microscope. Ultrathin sections, 60 nm thick, were cut from selected areas and contrasted with uranyl acetate and lead citrate. They were examined under a Philips CM120 TEM equipped with a Gatan Orius CCD camera (Philips, UK).

RT-PCR

Samples of liver were collected from 3 groups of fish selected as follows: (a) 17 clinically sick fish, (b) 10 asymptomatic fish from the same farm, and (c) 6 unexposed healthy control tilapia (also *O. niloticus*) from Grenada. Tilapia were deeply anaesthetized with tricaine methane sulfonate (MS-222; Syndel, Canada) and a total spinal cord severance was performed post-anesthesia. After dissection of the liver, all samples were individually placed in RNA-later (Qiagen, UK). Samples were kept at −20°C while not in transport. The RNA extractions were performed using RNeasy minikit (cat # 74104; Qiagen, UK) as directed by the manufacturer. A 1-step RT-PCR (Qiagen, UK) assay was conducted using degenerate primers *NM-CLU7-SF1*, *AGTTGCTTCT-CAYAAGCCTGCTA*, and *NM-CLU7-SR1*, *TCGTGTTCACARC-CAGGTTTACTT* to amplify a ~245-nucleotide region of the TiLV (Accession no. KJ605629). The RT-PCR conditions were 50°C for 30 minutes, 94°C for 15 minutes, and 35 cycles of 94°C for 30 seconds, 58°C for 30 seconds, and 72°C for 1 minute, with a final extension of 72°C for 5 minutes. Amplicons were visualized by electrophoresis in 1.5% agarose gels stained with ethidium bromide under ultraviolet light. Negative controls for RNA extraction and RT-PCR assays (SGU fish and water) were included in each assay. The PCR products were visualized on 2% agarose gel, purified with Purelink Gel Extraction kit (Invitrogen), and confirmed for target specificity by sequencing of both strands by Sanger Sequencing (GeneWiz, NJ). Negative controls for RNA extraction and RT-PCR assays (Tilapia bred and cultured at St George's University recirculating water facilities, Grenada) were included in each assay.

Results

RT-PCR

All liver samples from clinically sick fish were RT-PCR positive (17/17), while no amplicons were detected in liver samples from asymptomatic fish (0/10) or any of the Grenada controls (0/6). After trimming the primer sequences, 190-nt-long PCR fragments from 17 positive Ecuadorian fish, samples were aligned with published TiLV fragment (Accession no. KJ605629). Sequences showed 98%–100% nucleotide identity with reference sequences and positive samples.

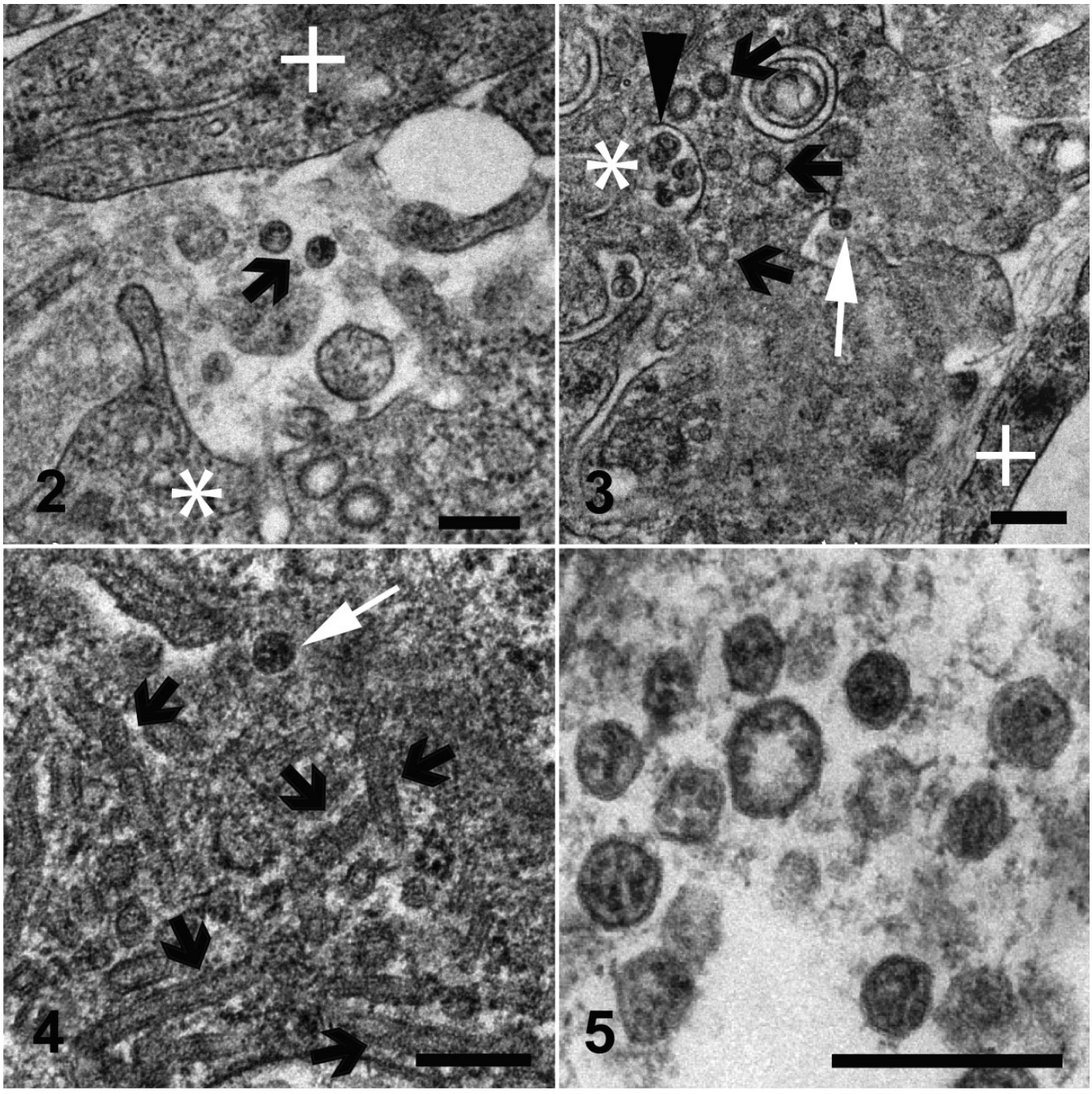

Figures 2–5. Three distinct virion morphologies, syncytial hepatitis of tilapia, liver, tilapia. Transmission electron microscopy. Scale bars: 200 nm. **Figure 2.** Nonenveloped free virions within the space of Disse (black arrow). **Figure 3.** Free extracellular virion (white arrow) and intracellular nonenveloped virions within intracytoplasmic membrane-bound vacuoles (black arrow). **Figure 4.** Free extracellular virion (white arrow) and filamentous/tubular extracellular virions (black arrow). *=hepatocyte, += endothelium. **Figure 5.** High-magnification image of the most commonly seen intracellular virion form, which lacks an envelope and may contain up to 7 electron-dense irregular aggregates within a core delimited by a trilaminar capsid.

Transmission Electron Microscopy

Virions were seen both within the cytoplasm of hepatocytes and in the space of Disse. Although occasionally icosahedral in appearance (Figs. 2–5), most virions noted were round and 60–100 nm in diameter (mean = 75 nm). They presented with variably retained structural detail (Fig. 5). When the structure was clearly visible, it featured a moderately electron-dense core containing several (up to 7) irregular electron-dense aggregates bounded by a trilaminar capsid.

Virions were seen to have at least 2 additional morphologies: round to oval enveloped structures and filamentous/tubular forms (Figs. 3 and 4). Enveloped virions were 70–110 nm wide (average = 100 nm), they had a moderately electron-dense core, a trilaminar capsid-like structure, and a 10- to 15–nm-thick moderately electron-dense external band containing regularly spaced electron-dense structures (envelope). Filamentous/tubular forms were less common, but when present they were 90–110 nm wide, of varying length, and had a moderately electron-dense core, a trilaminar capsid, and an envelope similar to that described above.

Multifocal invaginations of the cytoplasmic membrane containing virions were frequently seen at the sinusoidal pole of hepatocytes. This was occasionally associated with an electron-dense band below the membrane (vesicle formation with coating; Fig. 7).

The intracellular location of the virions is shown in Figs. 6–9. In most instances, virions were present within membranous intracytoplasmic structures morphologically consistent with endosomes located below the plasma membrane and at the central region of the cytoplasm. Conversely, in perinuclear areas, virions were contained within prominent membrane-bound anastomosing cisternae. Morphologically, these resemble greatly enlarged Golgi apparatus (Fig. 9). More rarely, virions were noted free floating within the cytoplasm.

Affected hepatocytes featured several additional pathological changes (data not shown). These included scattered, intracytoplasmic lattices of electron-dense material, some of which were membrane delimited. Other features included nucleolar dispersion, prominent nuclear pores, and intranuclear clusters of granular material. There was also multifocal hepatocyte necrosis, hepatocellular syncytial formation, hydropic degeneration, mitochondrial swelling, and the presence of intracytoplasmic lamellar bodies.

Discussion

The ultrastructural changes described here provide further evidence to support the previous suggestion of a viral etiology for SHT. Further confirmatory studies to isolate the virions and transmit this disease are required to confirm this. Several ultrastructural features of the virions shown in this article are similar to those of orthomyxoviruses. Moreover, preliminary RT-PCR data support the fact that the virus noted in SHT shows partial genetic homology (190 nucleotides) with TiLV, a novel RNA virus causing mortality in tilapia in Israel.[8]

The SHT targets the gastrointestinal tract as well as liver, but the ultrastructural component of this study has been restricted to the liver. Ultrastructurally, virions were noted only within hepatocytes and in the space of Disse and not within the endothelium. This suggests tropism of the SHT virus for the epithelial but not endothelial cell population in the liver. This ties in with the histological absence of sinusoidal disruption and hemorrhage, in contrast with ISA, where the causative isavirus is endotheliotropic.[15] A range of cell types has been shown to be infected by orthomyxoviruses. Influenza virus can infect respiratory epithelial cells, erythrocytes, leukocytes, and platelets,[5] whereas isavirus will target endothelium[15] but also leukocytes[20] and gill lamellar epithelium.[25] By contrast with SHT, isavirus has not been reported in necrotic hepatocytes,[20,24] although the isavirus (orthomyxovirus) associated with hemorrhagic kidney syndrome, in Canada, infected renal tubular epithelial cells,[4,18] suggesting that isavirus tropism for epithelial cells is possible in certain circumstances.

The ultrastructural features of the orthomyxoviral virion and replication cycle have been described in detail for several species, including influenza viruses[5] and isavirus.[4,15] The ultrastructural features of the virions noted in SHT are similar to those described for the above orthomyxoviruses. The electron-dense aggregates noted in the core of SHT-associated virus are similar to those previously described for influenza virus, which have been associated with the segmentation of the viral genome.[5] Moreover, extracellular tubular forms, similar to those noted in SHT, have been reported for both influenza virus[5] and isavirus.[15] The presence of an envelope at the extracellular stage has been described for influenza virus,[5] isavirus,[14,15] and TiLV virus.[8] By contrast, in our study, an envelope was not always seen in extracellular virions. The significance of this is unknown at this stage. Defective virions have been described for isavirus, and we cannot preclude the possibility of a similar situation in SHT-associated virus.[15]

In our study there were multiple instances of cytoplasmic membrane invagination containing virions, with occasional electron-dense coating, suggestive of virion endocytosis. We suspect that the process noted is similar to that previously observed in other orthomyxoviruses, where both clathrin-dependent and clathrin-independent endocytic mechanisms may be involved.[17] However, more work is required to ascertain this (eg, studies using double labelling for clathrin and SHT virions to assess hypothetical co-location). In influenza virus, endocytosis is followed by viral trafficking from early endosomes below the plasma membrane to perinuclear late endosomes. The latter have an acidic environment, and both influenza and isavirus have been shown to require a low pH step for release of their RNA into the cytoplasm.[7,16] In our SHT study, we noted intraendosomal virions below the plasma membrane but did not detect perinuclear, late endosomes.

Exceptionally for RNA viruses, orthomyxoviruses require nuclear involvement during their replication. This results in ultrastructural nuclear changes, including increase in nucleolar density, followed by dispersion and presence of granular material throughout the nucleus.[5] Sections of tilapia liver infected with SHT virus presented with nuclear dispersion, granular intranuclear material (occasionally clustered below the nuclear envelope), and prominence of nuclear pores. These nuclear features are similar to those described for orthomyxoviruses, although it is not feasible to discard the possibility that they are artefactual without more information on the features of the replication cycle of SHT-associated virions.

The final step in the viral replication cycle is exit from the host cell. In both influenza and isavirus, viral assembly takes place at the host cell cytoplasmic membrane by budding.[5,15]

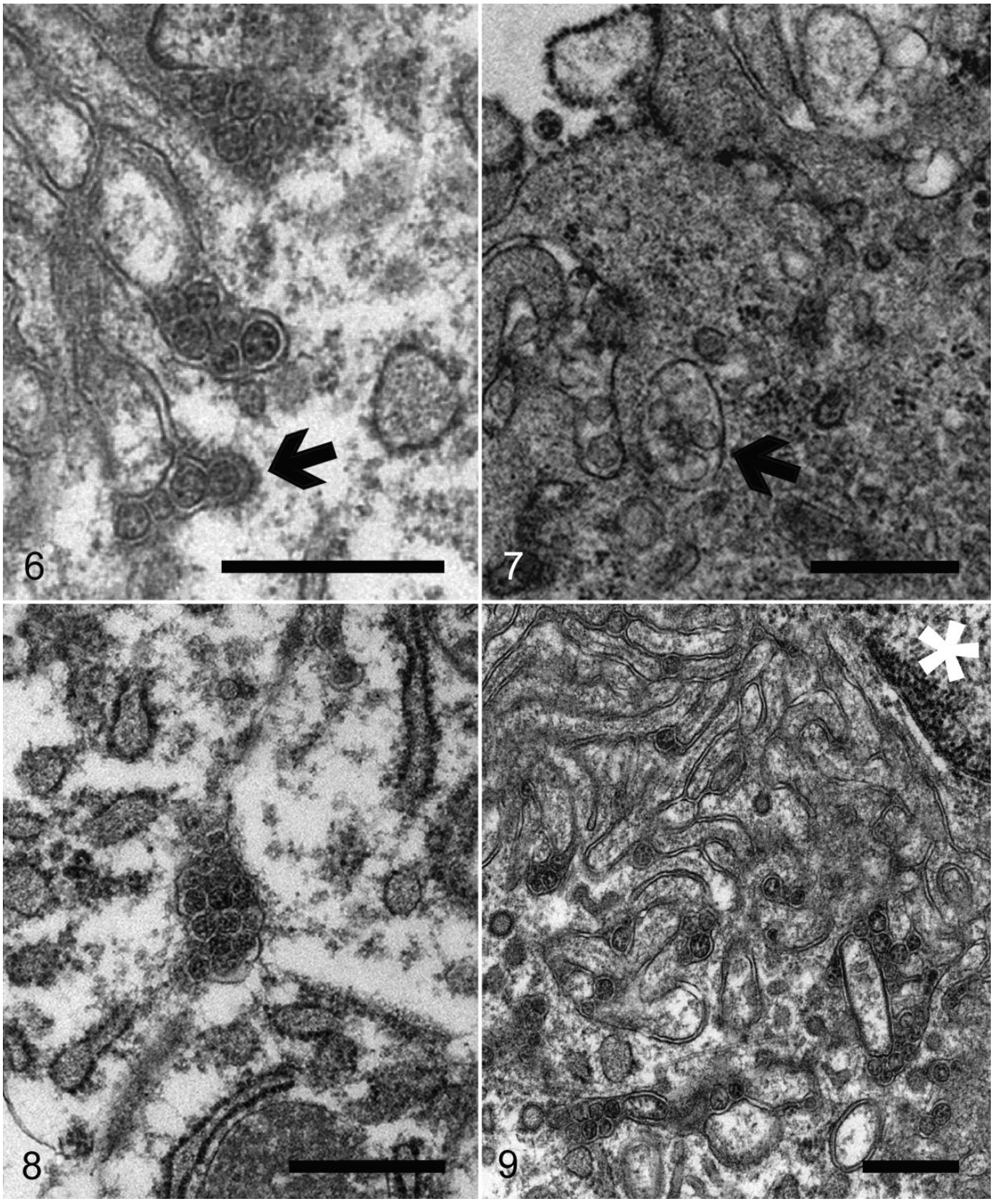

Figures 6–9. Syncytial hepatitis of tilapia, liver, tilapia. Transmission electron microscopy. Scale bars: 500 nm. **Figure 6.** Hepatocytes have multifocal invaginations of the cytoplasmic membrane. Note the electron-dense band below the membrane surrounding 1 of the virions (arrow). **Figure 7.** Intracytoplasmic virions are observed within membrane-bound structures consistent with endosomes below the plasma membrane (black arrow). **Figure 8.** Virions observed at the center of the cytoplasm. **Figure 9.** Intracytoplasmic virions observed within perinuclear cisternae; *=nucleus.

This is followed by release of the enveloped virus particle from the cell associated with the formation of long microvilli. Regrettably, instances of viral assembly and exit were not captured in the sections of this study on SHT, although there was disarray of hepatocyte villi at the sinusoidal pole. Further work is needed to characterize this.

So far, we have described ultrastructural features of SHT-associated virions that match those of described orthomyxoviruses. There are, however, several noteworthy areas of divergence. Perhaps the most notable of these is the presence of virions within a perinuclear complex of anastomosing membranous structures that are strongly suggestive of Golgi apparatus. The role and significance of this feature in the replication cycle of SHT-associated virus are unknown, but it is possible that this could represent an intracytoplasmic transport step of virions either toward the nucleus or toward the cytoplasmic membrane. There is a role for the Golgi apparatus in the replication cycle of influenza virus, where it participates in the transport of a subset of viral proteins to the plasma membrane,[5] but this does not feature intraluminal virions. Also the characteristic of SHT is the formation of syncytia, which is not a feature of orthomyxoviral infections. Syncytia formation, driven by a fusion factor, is reported in paramyxoviruses.[6] Finally, another noteworthy divergence is that in our sections we recorded free intracytoplasmic virions in SHT, which are not reported for orthomyxoviruses.[8] Overall, overlapping features with orthomyxovirus suggest it is possible to hypothesize that SHT-associated virions are novel orthomyxoviruses, but there are enough divergences to cast doubts over this possibility. Genome sequencing of SHT-associated virus is necessary to elucidate its taxonomy.

Above, we have discussed the ultrastructural features of SHT-associated virions. The published report of TiLV describes sparse electron-dense, 55–75 nm virions extra- and intracellularly in E-11 cell culture (from whole fry of snakehead).[8] Further examination of the pictures of TiLV published in this work (picture 2F)[8] reveals an ultrastructural morphology similar to SHT-associated virions (ie, intraendosomal location and capsid containing electron-dense aggregates). These similarities led us to test the probes published for TiLV on SHT clinical cases (and negative controls). Revealingly, the RT-PCR results do indeed confirm partial genetic homology between the virus noted in TSH and TiLV (190 nt). A complementary study has revealed further genetic homology.[1] These results highlight future research possibilities. For example, TiLV was isolated in E-11, a cell line originating from snakehead (*Ophicephalus striatus*) as well as in a primary tilapia brain cell culture.[8] E-11 is a clone of SSN-1, a cell obtained from whole fry (ie, composed of a mixed population).[13] It is therefore not unreasonable to assume that isolation of SHT virus may also be possible using E-11. This is despite possible differences in tissue tropism, as gross and histological diversity between TiLV and SHT also suggests. In TiLV, lesions include encephalitis and ophthalmitis with limited hepatic degeneration (hepatocellular pigment accumulation)[8]; conversely, in SHT there is hepatic necrosis with hepatocyte dissociation/syncytia formation and mucosal necrosis of gastrointestinal tract. This diversity may indicate these are distinct viruses, although it is noteworthy that differences in tissue tropism of 1 virus are possible. One example of this is isavirus: early descriptions of ISA in Norway featured hepatic lesions,[24] while in Canada the lesions were almost exclusively renal. In fact, the Canadian presentation was called hemorrhagic kidney syndrome before it was shown that the etiology was isavirus, albeit a strain different to that found in Norway.[4] Factors influencing tissue tropism include strain and age of fish and this may explain the enormous interstrain variation in susceptibility in SHT (from 90% for a farm-bred strain, "Chitralada," to 0% in a genetically all-male strain GMT; ie, genetically male tilapia).[9] In this outbreak, SHT was seen only in fry, which died very quickly. By contrast, TiLV was recorded in much larger fish, which experimentally survived for 7–10 days postinfection. Variation in tissue tropism due to age differences has been reported in a viral disease of salmon, infectious pancreatic necrosis ([IPN] caused by a birnavirus). In fry, IPN targets the liver, while in older fish the main lesions are pancreatic/gastrointestinal.[22] Concluding, the genetic homology noted between SHT-associated virus and TiLV represents only the initial stage of research into the link between these 2 viruses.

Overall, the results of the present study suggest that the virus associated with SHT is ultrastructurally similar to an orthomyxovirus, and that it presents with partial genetic homology with TiLV (190 nt). This homology has been confirmed further in a complementary study.[1] Further questions to be resolved include isolation of the virus, transmission studies, and further study of its replication cycle and pathogenesis.

Acknowledgments

The authors would like to acknowledge Stephen Mitchell at the electron microscopy unit of the University of Edinburgh for his help with TEM processing and viewing of the samples.

Declaration of Conflicting Interests

The author(s) declared no potential conflicts of interest with respect to the research, authorship, and/or publication of this article.

Funding

The author(s) received no financial support for the research, authorship, and/or publication of this article.

References

1. Bacharach E, Mishra N, Briese T, et al. Characterization of a novel orthomyxo-like virus causing mass die-offs of tilapia. *MBio*. 2016;**7**(2).
2. Bigarre L, Cabon J, Baud M, et al. Outbreak of betanodavirus infection in tilapia, *Oreochromis niloticus* (L.), in fresh water. *J Fish Dis*. 2009;**32**(8):667–673.
3. Blindheim S, Nylund A, Watanabe K, et al. A new aquareovirus causing high mortality in farmed Atlantic halibut fry in Norway. *Arch Virol*. 2015;**160**(1):91–102.
4. Byrne PJ, MacPhee DD, Østland VE, et al. Haemorrhagic kidney syndrome of Atlantic salmon, *Salmo salar* L. *J Fish Dis*. 1998;**21**(2):81–91.
5. Cheville NF, Lehmkuhl H. Orthomyxoviruses. In: Cheville NF, ed. *Ultrastructural Pathology*. Second ed. Ames, IA: Wiley-Blackwell; 2009: 356–357.
6. Cheville NF, Lehmkuhl H. Paramyxoviruses. In: Cheville NF, ed. *Ultrastructural Pathology*. Second ed. Ames, IA: Wiley-Blackwell; 2009:358–366.

7. Eliassen TM, Froystad MK, Dannevig BH, et al. Initial events in infectious salmon anemia virus infection: evidence for the requirement of a low-pH step. *J Virol*. 2000;**74**(1):218–227.
8. Eyngor M, Zamostiano R, Kembou Tsofack JE, et al. Identification of a novel RNA virus lethal to tilapia. *J Clin Microbiol*. 2014;**52**(12):4137–4146.
9. Ferguson HW, Kabuusu R, Beltran S, et al. Syncytial hepatitis of farmed tilapia, *Oreochromis niloticus* (L.): a case report. *J Fish Dis*. 2014;**37**(6):583–589.
10. Ghittino P. Viral hemorrhagic septicemia (VHS) in rainbow trout in Italy. *Ann N Y Acad Sci*. 1965;**126**(1):468–478.
11. Hedrick RP, Speas J, Kent ML, et al. Adenovirus-like particles associated with a disease of cultured white sturgeon, *Acipenser transmontanus*. *Can J Fish Aquat Sci*. 1985;**42**(7):1321–1325.
12. Isshik T, Nishizawa T, Kobayashi T, et al. An outbreak of VHSV (viral hemorrhagic septicemia virus) infection in farmed Japanese flounder *Paralichthys olivaceus* in Japan. *Dis Aquat Organ*. 2001;**47**(2):87–99.
13. Iwamoto T, Nakai T, Mori K, et al. Cloning of the fish cell line SSN-1 for piscine nodaviruses. *Dis Aquat Organ*. 2000;**43**(2):81–89.
14. Kibenge FS, Munir K, Kibenge MJ, et al. Infectious salmon anemia virus: causative agent, pathogenesis and immunity. *Anim Health Res Rev*. 2004;**5**(1):65–78.
15. Koren C, Nylund A. Morphology and morphogenesis of infectious salmon anaemia virus replicating in the endothelium of Atlantic salmon *Salmo salar*. *Dis Aquat Organ*. 1997;**29**(5):99–19.
16. Lakadamyali M, Rust MJ, Babcock HP, et al. Visualizing infection of individual influenza viruses. *Proc Natl Acad Sci U S A*. 2003;**100**(16):9280–9285.
17. Lakadamyali M, Rust MJ, Zhuang X. Endocytosis of influenza viruses. *Microbes Infect*. 2004;**6**(10):929–936.
18. Lovely JE, Dannevig BH, Falk K, et al. First identification of infectious salmon anaemia virus in North America with haemorrhagic kidney syndrome. *Dis Aquat Organ*. 1999;**35**(2):145–148.
19. Lovy J, Lewis NL, Hershberger PK, et al. Viral tropism and pathology associated with viral hemorrhagic septicemia in larval and juvenile Pacific herring. *Vet Microbiol*. 2012;**161**(1-2):66–76.
20. Moneke E, Groman DB, Wright GM, et al. Correlation of virus replication in tissues with histologic lesions in Atlantic salmon experimentally infected with infectious salmon anemia virus. *Vet Pathol*. 2005;**42**(3):338–349.
21. Plumb JA, Gaines JL, Mora EC, et al. Histopathology and electron microscopy of channel catfish virus in infected channel catfish, *Ictalurus punctatus* (Rafinesque). *J Fish Biol*. 1974;**6**(5):661–664.
22. Roberts RJ, Pearson MD. Infectious pancreatic necrosis in Atlantic salmon, Salmo salar L. *J Fish Dis*. 2005;**28**(7):383–390.
23. Shlapobersky M, Sinyakov MS, Katzenellenbogen M, et al. Viral encephalitis of tilapia larvae: primary characterization of a novel herpes-like virus. *Virology*. 2010;**399**(2):239–247.
24. Speilberg L, Evensen O, Dannevig BH. A sequential study of the light and electron microscopic liver lesions of infectious anemia in Atlantic salmon (Salmo salar L.). *Vet Pathol*. 1995;**32**(5):466–478.
25. Weli SC, Aamelfot M, Dale OB, et al. Infectious salmon anaemia virus infection of Atlantic salmon gill epithelial cells. *Virol J*. 2013;**10**:5.